Acta Crystallographica Section B
Structural Science
ISSN 0108-7681

Cis/*trans* isomers of PtX_2L_2 (*X* = halogen, *L* = neutral ligand); the crystal structure of *trans*-dichlorobis-(dimethyl sulfide)platinum(II) and the pressure dependence of its unit-cell dimensions

Christian Hansson,* Stefan Carlson,‡ Deborah Giveen, Maria Johansson,§ Shen Yong¶ and Åke Oskarsson

Department of Organic Chemistry, Centre for Chemistry and Chemical Engineering, Lund University, PO Box 124, SE-221 00 Lund, Sweden

‡ Current address: MAX-laboratory, Box 118, SE-221 00 Lund, Sweden.
§ Current address: Solid State Analysis, Astra-Zeneca R&D Mölndal, SE-431 83 Mölndal, Sweden.
¶ On leave from Zhongshan University, Guangzhou, People's Republic of China.

Correspondence e-mail: christian.hansson@inorg.lu.se

Received 20 October 2005
Accepted 7 February 2006

trans-$PtCl_2(dms)_2$ (dms is dimethyl sulfide) crystallizes in the space group $P2_1/n$ and adopts the molecular point group C_i, which is the most frequently occurring point group for *trans*-PtX_2L_2 complexes (78%), as observed in the Cambridge Structural Database (CSD; 2005 release), followed by C_1 (16%). Density functional theory calculations show that the observed geometry for *trans*-$PtCl_2(dms)_2$ has slightly higher energy than the most favorable geometry in the point group C_{2h}, but this geometry would require a space group that hampers close packing, thus showing that intermolecular forces determine the point group for the title compound. High-pressure powder diffraction studies of *trans*-$PtCl_2(dms)_2$ show no phase transformation up to 8.0 GPa. The bulk modulus is 8.1 (6) GPa and the pressure derivative 8.1 (4). In the CSD, the number of *cis*- and *trans*-PtX_2L_2 compounds are almost equal, *viz.* 156 *cis* and 160 *trans* compounds, showing no preference for either isomer in the solid state.

1. Introduction

A synthetic procedure resulting in a mixture of *cis*- and *trans*-$PtCl_2(dms)_2$ was published as early as 1934 (Cox *et al.*, 1934) and a tentative structure for the *trans* isomer, based on rotation X-ray photographs, was given. Horn *et al.* (1990) have determined the structure of the *cis* isomer but, besides a preliminary report (Johansson, 2001), no detailed structural model for the *trans* complex has been published previously.

Studies of the effects of high pressure on molecular crystals are at the initial stage but some characteristics have been reported, *i.e.* conformational changes and compression of weak intermolecular bonds (Boldyreva, 2003). As a result one can observe either a structural reconstruction, *i.e.* a phase transition, or a continuous distortion within the limits of stability of the same phase. No high-pressure investigation on *trans*-$PtCl_2(dms)_2$ has yet been published, and we present here a powder diffraction study up to 8.0 GPa.

Whether the formation of the *cis* and/or *trans* isomer of a complex is guided by thermodynamic and/or kinetic effects is an interesting and important question since the *cis* and *trans* isomers will have different properties. In many cases it is important to synthesize an isomerically clean product. In, for example, the Heck reaction it is the *cis* complex that goes into the catalytic cycle (Nilsson, 2005). Beck *et al.* (2002) have performed DFT (density functional theory) calculations on the structure and stability of some chelate complexes $[X(H_3P)Pt(N,O\text{-chelate})]$, X = Cl or CH_3, which exist in either *cis* or *trans* form (N donor with respect to the PH_3 ligand). They concluded that for $X = CH_3$ the *cis* isomer has slightly lower total energy than the *trans* isomer (1 kJ mol^{-1}), while the order is reversed for X = Cl (27 kJ mol^{-1}) in the gas phase

Table 1
Experimental details.

Crystal data	
Chemical formula	$C_4H_{12}Cl_2PtS_2$
M_r	390.25
Cell setting, space group	Monoclinic, $P2_1/n$
Temperature (K)	295 (2)
a, b, c (Å)	8.4637 (13), 6.0176 (10), 10.1812 (16)
α, β, γ (°)	90.00, 105.747 (3), 90.00
V (Å^3)	499.08 (14)
Z	2
D_x (Mg m^{-3})	2.597
Radiation type	Mo $K\alpha$
No. of reflections for cell parameters	2881
θ range (°)	2.8–31.8
μ (mm^{-1})	14.94
Specimen form, colour	Plate, yellow
Specimen size (mm)	0.28 × 0.12 × 0.06
Data collection	
Diffractometer	Bruker SMART CCD
Data collection method	ω scans
Absorption correction	Empirical
T_{min}	0.111
T_{max}	0.321
No. of measured, independent and observed reflections	5797, 1553, 1018
Criterion for observed reflections	$I > 2\sigma(I)$
R_{int}	0.081
θ_{max} (°)	31.8
Range of h, k, l	$-12 \Rightarrow h \Rightarrow 12$ $-8 \Rightarrow k \Rightarrow 8$ $-14 \Rightarrow l \Rightarrow 14$
Refinement	
Refinement on	F^2
$R[F^2 > 2\sigma(F^2)]$, $wR(F^2)$, S	0.046, 0.109, 0.96
Reflection/profile data	1553
No. of parameters	43
H-atom treatment	Constrained to parent site
Weighting scheme	$w = 1/[\sigma^2(F_o^2) + (0.060P)^2]$, where $P = (F_o^2 + 2F_c^2)/3$
$(\Delta/\sigma)_{max}$	<0.0001
$\Delta\rho_{max}$, $\Delta\rho_{min}$ (e Å^{-3})	1.78, −2.62

Computer programs used: *SMART* (Bruker, 1995), *SAINT-Plus* (Bruker, 1998), *SHELXS*97 (Sheldrick, 1997*a*), *SHELXL*97 (Sheldrick, 1997*b*), *DIAMOND* (Brandenburg, 2000).

and at 0 K. These findings stimulated us to search the Cambridge Structural Database (CSD; 2005 release; Allen, 2002) for one class of compounds, PtX_2L_2 (X is one and the same halogen and L is one and the same neutral ligand), to investigate the distribution of the *cis* and *trans* isomers. However, one must be cautious when attempting to derive regularities from such data, since they represent the existing set of crystal structures, and any observed trend may change in the future. In order to investigate the relative stabilities of the isomers we have performed DFT calculations in the gas phase optimizing the geometry of those complexes observed as both *cis* and *trans* isomers in the solid state in the CSD.

We have applied the question put forward by Brock & Dunitz (1994) – 'Exactly what molecular symmetries are retained in the crystal?' – to *trans*-PtX_2L_2, with potential C_i symmetry. Most of these complexes have potential C_{2h} symmetry, but some compounds may also contain stereoisomers not adopting C_i symmetry. We have screened the CSD for the crystal class distribution (Belsky *et al.*, 1995), which contains information about molecular point-group symmetry.

2. Experimental

2.1. Synthesis

trans-$PtCl_2(dms)_2$ was synthesized by the method of Cox *et al.* (1934). $K_2[PtCl_4]$ (1.0005 g, 2.4103 mmol) was dissolved in water (20 ml) in an ice-bath. Dimethyl sulfide (0.40 ml, 5.47 mmol) was added and the reaction mixture was stirred for 16 h. The light-yellow precipitate was filtered off and washed with water (3 × 5 ml). The precipitate was dried and then treated with ice-cold chloroform in order to extract $PtCl_2(dms)_2$. The insoluble part of the precipitate {*i.e.* $[Pt(dms)_4][PtCl_4]$} was filtered off and the chloroform was then allowed to evaporate.

The product was recrystallized from acetone. From the mixture of crystals of both *cis*- and *trans*-$PtCl_2(dms)_2$ a yellow monoclinic plate of *trans*-$PtCl_2(dms)_2$ was selected.

2.2. X-ray measurements and structure determination

Intensity data were collected on a Siemens Bruker SMART CCD diffractometer equipped with a rotating anode (Mo $K\alpha$ radiation, wavelength 0.71073 Å) at 295 K using exposure times of 20 s per frame. A total of 2300 frames were collected with ω scans and a frame width of 0.2°. The *SMART* software (Siemens, 1995) was used for the data collection. Completeness of 99.8% was accomplished out to θ = 30.1°. The first 50 frames were recollected at the end of the data collection to check for decay. No decay was observed.

The intensities were merged and integrated with *SAINT-Plus* (Siemens, 1998), and the effects of absorption were corrected using *SADABS* (Sheldrick, 1996). Structure determination was performed with Patterson and difference Fourier methods and refinement by full-matrix least-squares calculations using *SHELXL*97 (Sheldrick, 1997*b*). H-atom positions were calculated as riding on the adjacent C atom (methyl group C—H distance 0.96 Å), while non-H atoms were refined anisotropically. Figures of the complex and its packing arrangement were prepared using *DIAMOND* (Brandenburg, 2000).

Experimental details and crystal data are shown in Table 1.[1]

2.3. High-pressure experiments

High-pressure powder diffraction data were collected at Beamline I711, MAX-lab synchrotron source, Lund, Sweden (Cerenius *et al.*, 2000), using diamond–anvil cell (DAC) techniques [see *e.g.* Eremets (1996) for a full review]. The beam was monochromated and focused, and finally the spot size on the sample was reduced by the MAR Desktop slit system to 0.1 × 0.1 mm^2. Calibration of the wavelength (λ = 0.9264 Å) and sample–detector distance (d = 120 mm) was performed

[1] Supplementary data for this paper are available from the IUCr electronic archives (Reference: RY5001). Services for accessing these data are described at the back of the journal.

Table 2
Cell parameters of the title compound at different pressures.

Pressure (GPa)	*a* (Å)	*b* (Å)	*c* (Å)	β (°)	Volume (Å^3)
0.0001	8.4860 (6)	6.0353 (6)	10.2175 (8)	105.716 (6)	503.73 (5)
0.1370	8.4061 (5)	6.0034 (5)	10.1606 (6)	105.829 (6)	493.31 (4)
0.4110	8.3155 (9)	5.9607 (8)	10.112 (1)	106.02 (1)	481.8 (1)
0.8490	8.1889 (8)	5.9050 (6)	10.010 (1)	106.349 (8)	464.47 (8)
2.2190	7.963 (1)	5.7915 (8)	9.820 (1)	106.93 (1)	433.3 (1)
3.0410	7.867 (1)	5.7418 (7)	9.735 (1)	107.300 (9)	419.83 (9)
3.5890	7.8065 (7)	5.7061 (4)	9.6871 (7)	107.409 (6)	411.74 (6)
4.2740	7.7447 (7)	5.6735 (5)	9.6219 (7)	107.559 (7)	403.08 (6)
5.3980	7.6626 (7)	5.6223 (4)	9.5448 (7)	107.815 (7)	391.48 (6)
5.8090	7.6343 (8)	5.6073 (4)	9.5122 (7)	107.911 (7)	387.46 (6)
6.3020	7.5999 (7)	5.5911 (4)	9.4814 (7)	107.995 (7)	383.18 (5)
7.1790	7.5511 (7)	5.5626 (4)	9.4311 (7)	108.221 (8)	376.28 (6)
7.4800	7.5316 (7)	5.5530 (4)	9.4148 (8)	108.253 (8)	373.94 (6)
8.0010	7.5335 (8)	5.5545 (4)	9.4126 (9)	108.256 (9)	374.04 (6)

using powder diffraction data from LaB_6 powder in a capillary. The software *FIT2D* (Hammersley, 1997) was used in all data integration and calibration procedures. A Marresearch 165 mm 2000 × 2000 pixels CCD (Marresearch, 2002) was used to collect complete powder diffraction rings from samples, contained in a membrane-driven DAC (DXR-6, Diacel Products).

A well grounded powder sample of *trans*-$PtCl_2(dms)_2$ was loaded into the gasket hole (0.15 mm diameter and 0.1 mm deep), together with a small ruby crystal for pressure measurement and the methanol/ethanol (4:1) pressure transmitting medium. Pressure was calibrated by laser-induced fluorescence in the ruby crystal (Piermarini *et al.*, 1975). The pressure dependence of the *R*1 peak shift, calibrated by Mao *et al.* (1986), was used to estimate the pressure inside the DAC. The experiments were performed with the DAC mounted on a special stage fitted between the slit system and the CCD of the MAR Desktop. The sample-to-CCD distance was checked by a motorized rotation of the DAC to face a microscope perpendicular to the X-ray beam; this apparatus was used simultaneously for optical inspection and pressure determination by laser-induced ruby fluorescence. Thus, the DAC did not have to be removed from the experimental setup when increasing the pressure, which ensures a good reproducibility in the sample-to-detector distance.

Data were collected at 12 increasing pressures up to 8 GPa and two pressures when decreasing to ambient conditions. No phase transitions were observed, and the unit-cell dimensions appeared to be fully recovered when decreasing from 8 GPa to ambient pressure. Unit-cell dimensions were obtained from the powder diffraction data by using a combination of *WinPlotr* (Roisnel & Rodriguez-Carvajal, 2001) and *TREOR* (Werner *et al.*, 1985). Finally, a Le Bail-type peak-fitting procedure (Le Bail *et al.*, 1988) was performed in *GSAS* (Larson & Von Dreele, 1994) before refining the unit-cell dimensions. Powder diffraction data have been deposited in CIF format. Unit-cell parameters are given in Table 2 and in Figs. 1 and 2.

2.4. DFT calculations

Quantum chemical geometry optimizations were performed with the density functional method at the s-VWN level, as implemented in the *Turbomole*5.5 software (Alrichs *et al.*, 1989). Two models were used: one with a combination of larger basis sets (6-31g* for the lighter atoms hydrogen, carbon, nitrogen and oxygen, def-TZVPP for platinum, and TZVPP for all other atoms) and another with a combination of smaller basis sets [default in *Turbomole 5.5*; SV(P) for all atoms but hydrogen and ECP for platinum].

Results are given in Tables 3 and 4.

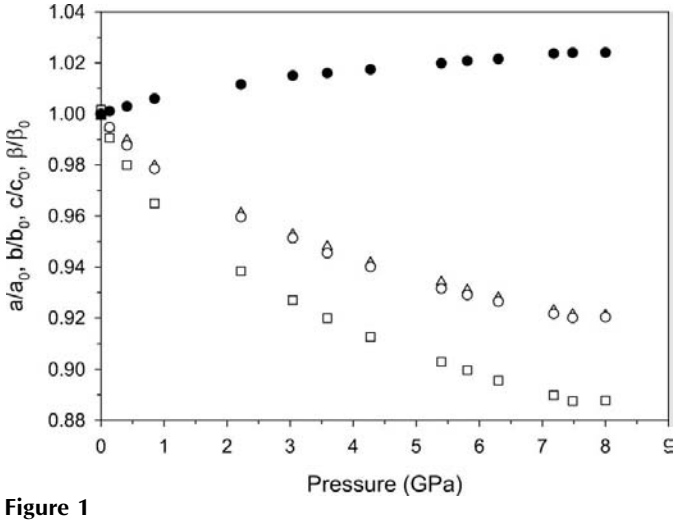

Figure 1
The relative change in unit-cell parameters *versus* pressure. Open squares, circles and triangles represent the *a*, *b* and *c* axes, respectively. Filled circles represent the β angle. The parameters at ambient pressure which were used for the normalization were a_0 = 8.4860 (7), b_0 = 6.0353 (6), c_0 = 10.2175 (1) Å and β_0 = 105.716 (6)°.

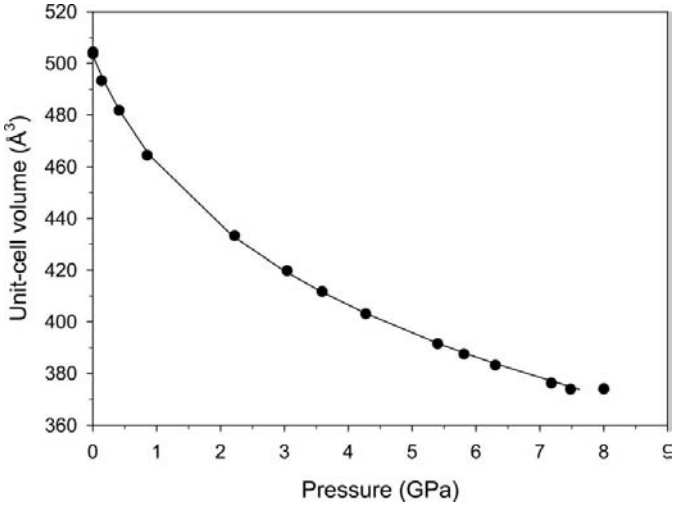

Figure 2
The pressure dependence of the unit-cell volume. The solid line represents a fit of the Vinet equation-of-state. The refined parameters V_0, K_0 and K_0' are 503 (2) Å^3, 8.1 (6) GPa and 8.1 (4), respectively.

Table 3
Calculated energy differences for compounds existing as both *cis* and *trans* isomers found in the CSD.

The first column is based on the larger basis set combination and the second on the smaller basis set combination (see §2).

Compound	$E_{trans} - E_{cis}$ (kJ mol^{-1})	$E_{trans} - E_{cis}$ (kJ mol^{-1})
$PtCl_2(dms)_2$	−18.1	−19.7
$PtCl_2(py)_2$	−41.9	−41.9
$PtCl_2(MeCN)_2$	−19.5	−13.2
$PtCl_2(EtCN)_2$	−18.0	−10.3
$PtCl_2(PhCN)_2$	−16.2	2.4
$PtCl_2(NH_2\text{-}cBu)_2$	−47.3	−46.3
$PtCl_2(tx)_2$	−17.2	−11.9
$PtCl_2(Ph_2S)_2$	−1.3	13.5
$PtCl_2[S{=}C(OEt)(NMe_2)]_2$	1.0	3.0
$PtCl_2(Pr_2SO)_2$	15.8	15.8
$PtCl_2(PPh_3)_2$	16.5	15.8
$PtCl_2(AsPh_3)_2$	11.1	11.8

3. Results and discussion

The CSD was searched using the *ConQuest* software (Bruno *et al.*, 2002) for compounds belonging to the class of mononuclear complexes PtX_2L_2, where X is a halogen and L is a ligand with a donor atom belonging to groups 14, 15 or 16. Simple solvates are included but no chelates are included, and eight structures with no coordinates, obscure connectivity or disorder have been excluded. There are 156 *cis* complexes and 160 *trans* complexes (deposited material), which may be regarded as a fairly large data set, indicating that there is no preference for either of the two isomers in the solid state.

The next step in the analysis was to choose compounds in the CSD that are reported as both *cis* and *trans* isomers, optimize the geometries with DFT calculations, using the crystallographically observed geometry as the starting geometry, and compare the total energy of the optimized structures in the gas phase. We have found 12 compounds reported as both *cis* and *trans* complexes, and their energy differences are given in Table 3. There is no clear-cut *cis*/*trans* division; of the 12 complexes the larger basis set combination has eight *trans* complexes as the favoured complex in the gas phase at 0 K, while the smaller basis set combination favours six *trans* complexes. The densities for *trans*- and *cis*-$PtCl_2(MeCN)_2$ are equal, while for all the others the *trans* compound has a larger density, which may indicate that the crystallization process may favour the *trans* compounds.

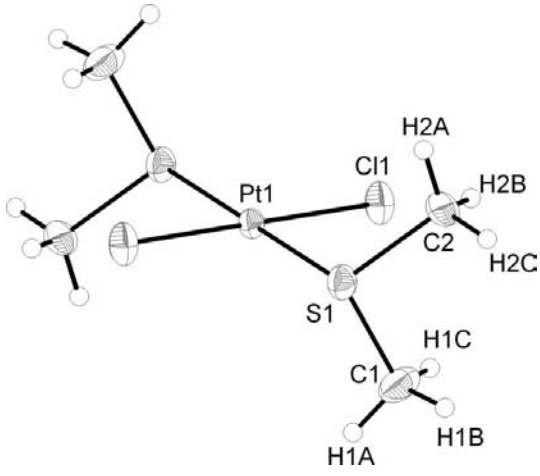

Figure 3
The atomic numbering scheme for *trans*-$PtCl_2(dms)_2$. Displacement ellipsoids are shown at the 30% probability level.

Table 4
Selected bond distances (Å), angles (°) and torsion angles (°) for *trans*-$PtCl_2(dms)_2$.

'Crystal' is the observed geometry in the solid state, C_{2h} is the structure optimized by DFT calculations with the larger basis set combination (see §2) using the crystal data as starting parameters and C_i is similar to C_{2h} but the torsion angles were fixed to those observed in the solid state. No symmetry constraints were used in the calculations.

	Crystal	C_{2h}	C_i
Pt1—Cl1	2.289 (2)	2.300	2.300
Pt1—S1	2.3024 (19)	2.288	2.286
S1—C1	1.799 (10)	1.794	1.792
S1—C2	1.778 (9)	1.794	1.793
Cl1—Pt1—S1	87.54 (8)	88.7	88.2
C2—S1—C1	98.8 (5)	98.7	100.3
C2—S1—Pt1	108.6 (3)	104.3	106.7
C1—S1—Pt1	105.2 (4)	104.8	103.2
Cl1—Pt1—S1—C1	−59.3 (5)	−51.7	−59.3
Cl1—Pt1—S1—C2	45.7 (4)	51.5	45.7

The title complex has a pseudo-square-planar geometry, *SP*-4–1 (Fig. 3), with Pt^{II} on an inversion centre, thus conforming to the molecular point group C_i, which is the highest allowed for the complex in the space group observed ($P2_1/n$). Other possible point groups, C_{2h}, C_{2v}, C_2 and C_s, do not conform to this space group. Relevant geometrical parameters from the crystal structure determination as well as two geometries in the gas phase optimized by DFT calculations are given in Table 4. There is a very good agreement between observed and calculated (in the gas phase) bond distances and angles (maybe with the exception of the C—S—Pt angles). The Cl—Pt—S—C angles show the largest discrepancies, which is not surprising since packing effects should have a large influence on these angles. The calculated geometry is not only close to C_i but also very close to the highest symmetry possible for the complex, C_{2h}. There are many energy minima in the conformational space, with energies fairly close to the minimum for the C_{2h} conformation shown in Table 4. A systematic study of the conformational space with starting parameters obeying C_i was performed changing the Cl—Pt—S—C torsion angles by 10° between each subsequent calculation. One minimum, with Cl—Pt—S—C angles of 10 and 115° for one-half of the molecule, is observed with an energy of only 2.3 kJ mol^{-1} above the lowest C_{2h} minimum. All calculations converged to either the lowest C_{2h} or to this minimum. In conclusion the observed conformation in the solid state is not at either the anticipated global (C_{2h}) or the local minimum, but slightly (5–7° for relevant torsion angles) off the global minimum. The energy difference between the lowest C_{2h} minimum and the observed geometry in the solid state is probably very small; a DFT optimization calculation starting from the crystal structure parameters and keeping the Cl—Pt—S—C torsion angles

fixed at the observed value resulted in an energy only 1.7 kJ mol^{-1} larger than the lowest C_{2h} minimum (the larger basis set combination was used). It is evidently more advantageous to crystallize in $P2_1/n$, which allows close packing (Kitaigorodsky, 1973), than in $P2/m$, which is required for the C_{2h} point group.

A comparison of the Pt—Cl and Pt—S distances in the two isomers as observed in the crystal structures shows that the Pt—Cl distances are 0.028 (3) Å longer and the Pt—S distances are 0.031 (3) Å shorter in the *cis* complex (Horn *et al.*, 1990). The differences are probably significant even when taking packing effects into account and show that sulfur has a larger *trans* influence than chlorine, which has been shown previously by Lövqvist (1996).

The packing of *trans*-$PtCl_2(dms)_2$ is shown in Fig. 4. The Pt^{II} centre forms an *I*-centred monoclinic unit cell, but the other atoms break the *I*-centring, thus giving a primitive unit cell. The complexes are stacked along the *b* axis, with agostic interactions Pt···H of 3.08 and 3.31 Å. These rows may be regarded as forming layers in the *bc* plane, which feature a ring of six methyl groups with soft H···H interactions of 2.68 and 2.97 Å. The Pt—Cl bond in the two adjacent layers points slightly off the inversion centre of the ring, with a Cl···Cl distance of 4.037 (3) Å. The five close Cl···H interactions on each side of a layer are in the range 2.96–3.28 Å. Mulliken analysis of the crystallographically observed geometry and the larger basis set combination resulted in Pt = −0.6, S = 0.4, Cl = −0.2 and CH_3 = 0.04 (the smaller basis-set combination gives Pt = −0.3, S = 0.2, Cl = −0.2 and CH_3 = 0.12). It is thus reasonable to assume that electrostatic interactions contribute to stabilizing the packing arrangement as manifested in the synthon –Cl···$(CH_3)_n$···Cl–. Most Pt^{II}–Cl complexes in the CSD have Cl···Cl distances in the interval 3.8–3.9 Å (deposited material), and it is assumed that there are no Cl···Cl contacts at ambient pressure.

The result of the high-pressure experiments is shown in Table 2 and in Figs. 1 and 2. There is a decrease of cell volume by 26% with no phase transformation when the compound is exposed to pressures of up to 8.0 GPa. One way of describing the compression of a material is to estimate its bulk modulus by fitting an equation-of-state (EOS) to the unit-cell volume data. After first testing the Murnaghan (1937) and Birch–Murnaghan (Birch, 1947) EOS, we found that the EOS of Vinet *et al.* (1986), derived from cohesive energies in condensed systems, best describes the *p*–*V* data. It can be expressed as

$$p = 3K_0 y^{-2/3}(1 - y^{-1/3}) \exp[3(K_0' - 1)(1 - y^{1/3})/2],$$

where $y = V/V_0$, and K_0, K_0' and V_0 are the bulk modulus, its pressure derivative and the unit-cell volume at ambient pressure, respectively. The parameters K_0, K_0' and V_0 were fitted to the unit-cell volume data using the software *EOSFIT*5.2 (Angel, 2001). The fitted bulk modulus, K_0 = 8.1 (6) GPa, is consistent with highly compressible materials such as molecular crystals. Comparable values are found for other molecular crystalline materials, *e.g.* lithium- and potassiumcyclopentadienide (Dinnebier *et al.*, 2005), for which K_0 was fitted to 8 and 5 GPa, respectively (K_0' = 7 and 11, respectively). The fitted pressure derivative for *trans*-$PtCl_2(dms)_2$ is K_0' = 8.1 (4) and describes a large curvature in the *p*–*V* data. For minerals a K_0' value of around 4 is frequently found, but for 'softer' materials, such as the cyclopentadienides mentioned above, higher values are common. Other examples are 4-(5-methyl-1,3,4-oxadiazole-2-yl)-*N*,*N*′-dimethylphenylamine (6.3 GPa and 6.8 for the bulk modulus and its pressure dependence, respectively) and 2,5-diphenyl-1,3,4-oxadiazole (7.3 GPa and 6.8; Franco *et al.*, 2002). The volume decrease in the title compound shows the largest effect on the *a* axis, *i.e.* perpendicular to the layers, and about the same for the *b* and *c* parameters, *i.e.* within the layers. This result would be explained if the Cl atoms move towards the ring formed by the methyl groups, thus successively filling the void in the ring. Now the Cl atoms must slide beside each other resulting in the β angle increasing with pressure, which is also observed (Table 2).

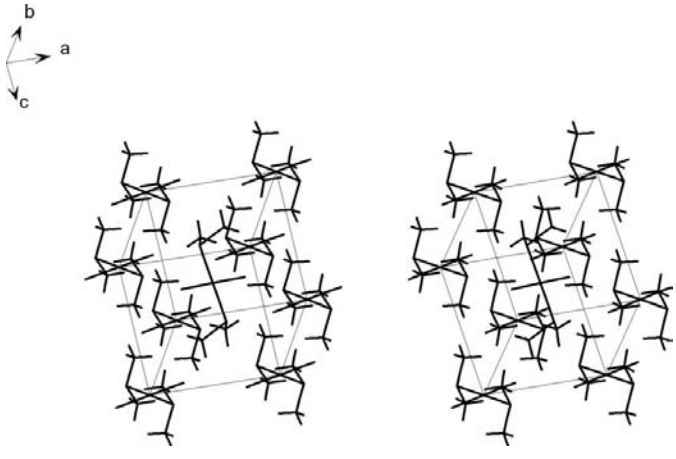

Figure 4
A stereoview of the packing arrangement of *trans*-$PtCl_2(dms)_2$.

trans-$PtCl_2(dms)_2$ retains the molecular point group C_i rather than the other possibilities, C_1, C_s, C_2, C_{2v} and C_{2h}, in the solid state. In order to investigate if the retention of C_i in the solid state is a general feature for *trans*-PtX_2L_2 complexes, we have investigated the 160 compounds found in the CSD. The structural class (Belsky *et al.*, 1995; Belsky & Zorkii, 1977) distribution for these compounds (deposited material) shows that the molecular symmetry C_i is retained in 78% of the structures (compared with 99% for structures in general in the CSD; Pidcock *et al.*, 2003), followed by C_1 (16%), C_2 (4%) and C_{2h} (2%). More than 60% of the complexes have potential C_{2h} molecular symmetry, but this symmetry is retained in only 2% of cases. Molecular symmetry C_{2h} requires platinum in crystallographic point symmetry 2/*m*, which is found in space groups that hamper close packing (Kitaigorodsky, 1973). Inversion centres thus seem to be especially favourable for crystal packing, as is also proposed by Brock & Dunitz (1994).

In conclusion, there is no preference in frequency of either *cis* or *trans* isomers of PtX_2L_2 compounds in the CSD (2005 release). The molecular point group C_i is retained in the crystal for 78% of reported *trans*-PtX_2L_2 complexes, followed

by C_1 with 16%. The high-pressure investigation shows that the unit-cell volume is decreased by 26% up to 8.0 GPa without any phase transition.

Financial assistance from the Crafoord Foundation, the Swedish Research Council and Lund University for a scholarship to SY is gratefully acknowledged. MAX-laboratory and Yngve Cerenius are acknowledged for the allocated beam time and technical support.

References

Allen, F. H. (2002). *Acta Cryst.* B**58**, 380–388.

Alrichs, R., Bär, M., Häser, M., Horn, H. & Kölmel, C. (1989). *Chem. Phys. Lett.* **162**, 165–169.

Angel, R. J. (2001). *High-Pressure, High-Temperature Crystal Chemistry*, edited by R. M. Hazen & R. T. Downs, p. 35. *Reviews in Mineralogy and Geochemistry*, Vol. 41. Washington, DC: Mineralogical Society of America.

Beck, W., Klapötke, T. M. & Ponikwar, W. (2002). *Z. Naturforsch. Teil B*, **57**, 1120–1124.

Belsky, V. K., Zorkaya, O. N. & Zorky, P. M. (1995). *Acta Cryst.* A**51**, 473–481.

Belsky, V. K. & Zorkii, P. M. (1977). *Acta Cryst.* A**33**, 1004–1006.

Birch, F. (1947). *Phys. Rev.* **71**, 809–824.

Boldyreva, E. (2003). *High-Pressure Induced Structural Changes in Molecular Crystals Preserving the Space Group Symmetry: Anisotropic Distortion/Isosymmetric Polymorphism.* INDABA IV 'Patterns in Nature', Skukuza, Kruger NP, South Africa.

Brandenburg, K. (2000). *DIAMOND*2. Crystal Impact, Bonn, Germany.

Brock, C. P. & Dunitz, J. D. (1994). *Chem. Mater.* **6**, 1118–1127.

Bruno, I. J., Cole, J. C., Edgington, P. R., Kessler, M., Macrae, C. F., McCabe, P., Pearson, J. & Taylor, R. (2002). *Acta Cryst.* B**58**, 389–397.

Cerenius, Y., Ståhl, K., Svensson, A., Ursby, T., Oskarsson, Å., Albersson, J. & Liljas, A. (2000). *J. Synchrotron Rad.* **7**, 203–208.

Cox, E. G., Saenger, H. & Wardlaw, W. (1934). *J. Chem. Soc.* pp. 182–186.

Dinnebier, R. E., van Smaalen, S., Olbrich, F. & Carlson, S. (2005). *Inorg. Chem.* **44**, 964–968.

Eremets, M. (1996). *High Pressure Experimental Methods.* Oxford University Press.

Franco, O., Reck, G., Orgzall, I. & Schulz, B. (2002). *J. Phys. Chem. Solids*, **63**, 1805–1813.

Hammersley, A. P. (1997). *FIT2D.* ESRF Internal Report, ESRF97HA02T: An Introduction and Overview. ESRF, Grenoble, France.

Horn, G. W., Kumar, R., Maverick, A. W., Fronczek, F. R. & Watkins, S. F. (1990). *Acta Cryst.* C**46**, 135–136.

Johansson, M. (2001). PhD thesis, Lund University, Sweden.

Kitaigorodsky, A. I. (1973). *Molecular Crystals and Molecules*, ch. 1. New York/London: Academic Press.

Larson, A. C. & Von Dreele, R. B. (1994). LANSCE MS-H805. Los Alamos National Laboratory, New Mexico, USA.

Le Bail, A., Duroy, H. & Fourquet, J. L. (1988). *Mater. Res. Bull.* **23**, 447–452.

Lövqvist, K. (1996). PhD thesis, Lund University, Sweden.

Mao, H. K., Xu, J. & Bell, P. M. (1986). *J. Geophys. Res.* **91**, 4673–4676.

Marresearch (2002). Marresearch GmbH, Norderstedt, Germany.

Murnaghan, F. D. (1937). *Am. J. Math.* **49**, 235–260.

Nilsson, P. (2005). PhD thesis, Lund University, Sweden.

Pidcock, E., Motherwell, W. D. S. & Cole, J. C. (2003). *Acta Cryst.* B**59**, 634–640.

Piermarini, G. J., Block, S., Barnett, J. D. & Forman, R. A. (1975). *J. Appl. Phys.* **46**, 2774–2780.

Roisnel, T. & Rodriguez-Carvajal, J. (2001). *Mater. Sci. Forum*, **378–381**, 118123.

Sheldrick, G. M. (1996). *SADABS.* University of Göttingen, Germany.

Sheldrick, G. M. (1997*a*). *SHELXS*97. University of Göttingen, Germany.

Sheldrick, G. M. (1997*b*). *SHELXL*97. University of Göttingen, Germany.

Siemens (1995). *SMART.* Bruker Analytical X-ray Instruments Inc., Madison, Wisconsin, USA.

Siemens (1998). *SAINT-Plus.* Bruker Analytical X-ray Instruments Inc., Madison, Wisconsin, USA.

Vinet, P., Ferrante, J., Smith, J. R. & Rose, J. H. (1986). *J. Phys. C*, **19**, L467–L473.

Werner, P.-E., Eriksson, L. & Westdahl, M. (1985). *J. Appl. Cryst.* **18**, 367–370.